

---

# Self-Supervised Spatial-Temporal Feature Learning for Video Correspondence

---

Anonymous Author(s)

Affiliation

Address

email

## Abstract

1 Learning a generalizable representation for video correspondence is a vital problem  
2 for various computer vision tasks. A variety of self-supervised pretext tasks  
3 are proposed to address the problem from different perspectives. In this paper,  
4 we decouple the video correspondence learning into two parts, including spatial  
5 and temporal feature learning. While spatial feature learning is realized using  
6 contrastive loss with unlabeled image data, we perform temporal feature learning  
7 in the regime of frame reconstruction to estimate motion between video frames.  
8 To address the issues of catastrophic forgetting and temporal discontinuity when  
9 training with video data, we design a pyramid learning framework with local  
10 and global correlation distillation, which facilitates fine-grained matching while  
11 maintaining the capability of capturing object appearance. Our method surpasses  
12 the state-of-the-art self-supervised methods on a series of correspondence-related  
13 tasks. The detailed ablation study further verifies the effectiveness of our approach.

## 14 1 Introduction

15 Learning representations for video correspondence is a fundamental problem in computer vision,  
16 which is closely related to different video applications, including optical flow estimation [7][14], video  
17 object segmentation [2][31], keypoint tracking [46], etc. However, supervising such a representation  
18 requires a large number of dense annotations, which is unaffordable. Thus most approaches acquire  
19 supervision from simulations or limited annotations, which result in poor generalization in different  
20 downstream tasks. Recently, self-supervised feature learning is gaining significant momentum, and  
21 several pretext tasks are designed for space-time visual correspondence using abundant unlabeled  
22 videos.

23 The key to this task lies in two different perspectives. The first one is **temporal feature learning**,  
24 which aims to learn the fine-grained correspondence of pixel between frames. With the nature of  
25 temporal coherence in the video, the temporal feature learning can be formed as a reconstruction  
26 task, where the query pixel in the target frame can be reconstructed by leveraging the information of  
27 adjacent reference frames with a local range. Then a reconstruction loss is applied to minimize the  
28 photometric error between the raw frame and its reconstruction. However, the temporal discontinuity  
29 occurs frequently due to the occlusions, dramatic appearance changes, and deformations, especially  
30 for pixels in each frame with large down-sampling. In such scenarios, the frame reconstruction  
31 loss apparently becomes invalid, which results in inferior performance. To alleviate the problem,  
32 MAST [20] applies frame reconstruction with a higher feature resolution by decreasing the stride of  
33 the backbone, which requires a larger memory and computation cost.

34 Another way to exploit free temporal supervision is by exploiting temporal cycle-consistency. [15][41]  
35 track objects forward and backward with the objective of maximizing the cycle-consistency using  
36 reconstruction and contrastive loss. However, compared to the correspondence learning which is

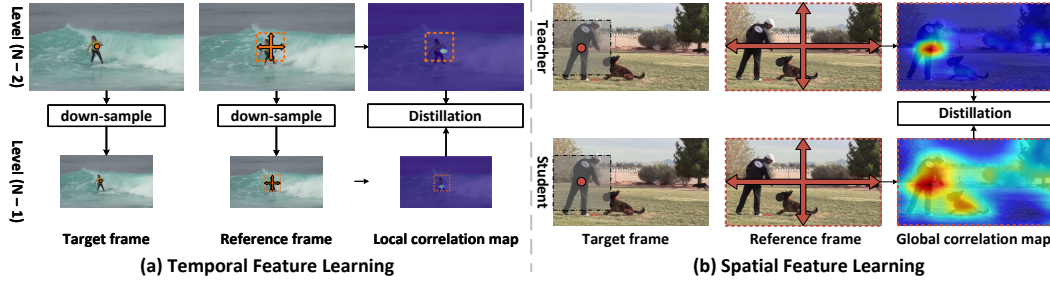


Figure 1: **Illustration of the main idea.** In (b), we first train a contrastive model on ImageNet [6] and fixed it as teacher. Then the distillation on global correlation map is proposed to maintain the ability to capture object appearance. In (a), the distillation is performed between local correlation maps at different pyramid levels to facilitate fine-grained matching. The local correlation map computed at lower pyramid level is regarded as pseudo labels.

37 realized at object-level, the frame reconstruction is conducted on raw image space, which provides  
 38 more accurate supervision for learning fine-grained correspondence.

39 The second one is **spatial feature learning**, which pays more attention to learning the object  
 40 appearance that is invariant to viewpoint and appearance changes. [39] adopts a novel intra-inter  
 41 consistency loss to learn discriminative spatial feature while [47] learns the space-time correspondence  
 42 through a frame-wise contrastive loss. Both methods are trained on video datasets and try to realize  
 43 the spatial and temporal feature learning in a unified framework, which is sub-optimal for each of  
 44 them. Recently, as mentioned in [43], the contrastive model [13][45] pre-trained on image data shows  
 45 competitive performance against dedicated methods for video correspondence due to its superior  
 46 capability of learning spatial representation. However, such a model still fails to realize the fine-  
 47 grained matching between video frames. This motivates us to design a framework that learns the  
 48 spatial and temporal features independently with image and video data.

49 In this paper, we decouple video correspondence learning into two separate processes, including  
 50 spatial and temporal feature learning. To achieve this, we first train the model in a contrastive learning  
 51 paradigm on ImageNet [6], which gives the model the ability to capture object appearance. Then,  
 52 instead of training with a large video dataset, *i.e.*, Kinetics [4] with 300k videos, we perform the  
 53 temporal feature learning on YouTube-VOS [48], which consists of 3.5k videos. However, apart  
 54 from the severe information loss and temporal discontinuity due to large spatial down-sampling on  
 55 frames, directly fine-tuning the old model with only new data will leads to a well-known phenomenon  
 56 of catastrophic forgetting [22]. To address the first problem, we propose a novel pyramid learning  
 57 framework. The frame reconstruction is applied at different levels of the network to better exploit the  
 58 free temporal supervision. As you can see in Figure 1 (a), the pixels of the target and reference frame  
 59 with higher resolution have a lower chance of occurring temporal discontinuity, which provides a  
 60 more accurate local correlation map. Thus we design a new loss named local correlation distillation  
 61 loss that supports explicitly learning of the correlation map in the region with high uncertainty, which  
 62 is achieved by taking the finest local correlation map as pseudo labels. At the same time, as shown  
 63 in Figure 1 (b), we freeze the model pre-trained on ImageNet as teacher. Then a global correlation  
 64 distillation loss is proposed to keep the student the ability to capture object-level correspondence,  
 65 which is closely related to object appearance modeling.

66 To sum up, our main contributions include: (a) We propose a decoupled learning paradigm for self-  
 67 supervised video correspondence, including spatial and temporal feature learning. (b) We propose a  
 68 pyramid learning framework with local correlation distillation to improve the capability of estimating  
 69 fine-grained correspondence. (c) We introduce a global correlation distillation loss to keep the ability  
 70 to capture object appearance when training on a video dataset. (d) Last but not least, we verify our  
 71 approach in a series of correspondence-related tasks, including video object segmentation, human  
 72 parts propagation, and pose tracking. Our approach consistently outperforms previous state-of-the-art  
 73 self-supervised methods and is even comparable with some task-specific fully-supervised algorithms.

## 74 2 Related Work

75 **Self-supervised learning for video correspondence.** Recent approaches focus on learning cor-  
 76 respondence from unlabeled videos in a self-supervised manner. The task requires the model to

have the ability to capture object appearance and estimate the fine-grained correspondence between frames at the same time, which has proceeded along two different dimensions: reconstruction-based methods [19][20][21][38][39] and cycle-consistency-based methods [15][41][52]. In the first type, a query point is reconstructed from adjacent frames while the latter performs forward-backward tracking with the objective of minimizing the cycle inconsistency. Through getting promising results, most methods address the problem by considering only one perspective. VFS [47] learns the spatial and temporal representation through a frame-wise contrastive loss while [1][39] try to realize the spatial and temporal feature learning in a unified framework by exploiting the inter-video constraint, which may result in sub-optimal performance. In this paper, we learn a better representation by decoupling the video correspondence learning into two separate processes, including spatial and temporal feature learning.

**Self-supervised spatial feature learning.** Self-supervised spatial feature learning aims to learn discriminative features of object appearance with unlabeled data, which recently got promising result with contrastive learning. In an early work [44], the contrastive learning is formulated as an instance discrimination task, which requires the model to return low values for similar pairs and high values for dissimilar pairs. Recently, the performance is further improved by creating a dynamic memory-bank [13], introducing online clustering [3] and avoiding the use of negative pairs [5][11]. Furthermore, [42][45][49] propose various pre-text tasks to adapt the contrastive learning to tasks which require dense prediction. Even though showing superior performance for video correspondence learning [43], the contrastive model pre-trained on image data still struggles to model the fine-grained correspondence between video frames.

**Self-supervised temporal feature learning.** Compared to spatial feature learning, temporal feature learning focus on learning the motion information of video, which is closely related to optical flow and motion estimation. Most methods [7][34] directly regress the ground-truth optical flow produced by synthetic datasets, thus suffering from severe domain shift. To deal with the problem, [28] tries to learn the dense correspondence on real video without any label by minimizing the photometric error between the raw frame and its reconstruction in the valid region. However, the video frames usually contain temporal discontinuity including dramatic appearance changes and occlusions, which seriously degrades the capability of the method. [18][24][25] alleviate the problem by utilizing the optical flow predictions from teacher model to guide the learning of student model in the region with occlusions. In this paper, we address the issue from two perspectives: (1) Learning a better representation that is invariant for object appearance changes. (2) Supervising the correlation by taking the finest correlation as pseudo labels.

### 3 Approach

The basic idea of our method is to decouple video correspondence learning into two separate processes, including spatial and temporal feature learning. We first train our model using contrastive loss with image data to learn the object appearance that is invariant to appearance changes. Then, we perform the temporal feature learning on a small video dataset to learn the fine-grained correspondence between frames. In order to deal with the problems including temporal discontinuity and catastrophic forgetting, a pyramid learning framework is proposed with local and global correlation distillation.

#### 3.1 Spatial Feature Learning

The spatial feature mainly describes the appearance of objects involved in an image. Spatial feature learning is analogous to that of instance discrimination and thus easily benefits from the recent advancements brought by contrastive learning. We first briefly review the instance discrimination objective in contrastive learning. Given an encoded query  $\mathbf{q} \in \mathbb{R}^d$  and a set of encoded key vectors  $\mathcal{K} = \{\mathbf{k}^+, \mathbf{k}_1^-, \mathbf{k}_2^-, \dots, \mathbf{k}_K^-\}$  which consists of one positive key  $\mathbf{k}^+ \in \mathbb{R}^d$  and  $K$  negative keys  $\mathcal{K}^- = \{\mathbf{k}_j^-\}$ , where  $d$  denotes the embedding dimension. The query and its positive key are generated from the same instance with two different augmentations, while the negative keys refer to other instances. The objective of instance discrimination is to maximize the similarity between the query  $\mathbf{q}$  and the positive key  $\mathbf{k}^+$  while remaining query distinct to all negative keys  $\mathcal{K}^-$ . Thus, a contrastive loss is presented in InfoNCE [36] with a softmax formulation:

$$\mathcal{L}_{\text{ncc}} = -\log \frac{\exp(\mathbf{q}^T \mathbf{k}^+ / \tau_c)}{\exp(\mathbf{q}^T \mathbf{k}^+ / \tau_c) + \sum_{i=1}^K \exp(\mathbf{q}^T \mathbf{k}_i^- / \tau_c)}, \quad (1)$$

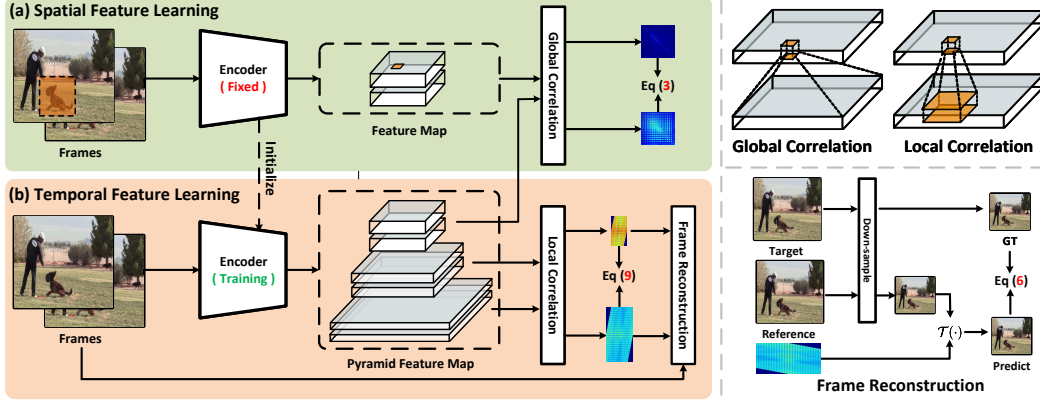


Figure 2: **An overview of our framework.** Our method decouples video correspondence learning into two separate processes, including spatial feature learning and temporal feature learning. Specifically, the spatial feature learning first exploits the contrastive loss, which is analogous to that of instance discrimination, to learn the object appearance with image data. Then we perform the self-supervised training with video data in the next step. To maintain the ability to capture object appearance, we fix the pre-trained network as teacher and a global correlation distillation is devised. For temporal feature learning, we propose a pyramid learning framework where the frame reconstruction is devised at each pyramid level of the network. At the same time, we introduce a novel loss named local correlation distillation loss that supports explicitly learning of the correlation map in the region with high uncertainty, which is achieved by taking the finest local correlation map as pseudo labels.

where the similarity is measured via dot product, and  $\tau_c$  is the temperature hyper-parameter. MoCo [13] builds a dynamic memory bank to maintain a large number of negative samples with a moving-averaged encoder. DetCo [45] further improves the contrastive loss  $\mathcal{L}_{nce}$  by introducing a global and local contrastive learning to enhance local representation for dense prediction. In this paper, we adopt the same framework as [13][45] to learn an appearance model for most of our experiments.

**Global correlation distillation.** After main training with contrastive loss, we get an encoder  $\phi$ . Then we continuously train it on video data to learn the fine-grained correspondence ( See section 3.2 ). However, directly fine-tuning the old model with only new data will lead to a well-known phenomenon of catastrophic forgetting [22], which degrades the performance. Thus we introduce a global correlation distillation loss in order to maintain the ability to capture object appearance. More specifically, we first fix the feature encoder  $\phi$  as teacher denoted as  $\phi_t$ . Given a pair of video frames consisting of target and reference frame  $I_t, I_r$ , the  $\phi$  maps them to a pair of feature embeddings  $F_t^l, F_r^l \in \mathbb{R}^{h^l w^l \times d^l}$ , where  $l \in \{0, 1, \dots, N\}$  is the index of each pyramid level and the smaller number represents the coarser pyramid level. Here  $l$  is set to  $N$ . For each query point  $F_t^l(i)$  and key point  $F_r^l(j)$ , we compute the global correlation  $a_{i,j}$  using a softmax over similarities *w.r.t.* all keys in the reference frame ( see the upper right of Figure 2 ), *i.e.*:

$$a_{i,j} = \frac{\exp(F_t^l(i) \cdot F_r^l(j)/\tau)}{\sum_n \exp(F_t^l(i) \cdot F_r^l(n)/\tau)}, i, j, n \in \{1, \dots, h^l w^l\}, \quad (2)$$

Where ‘ $\cdot$ ’ stands for the dot product. Each point in  $F_t^l$  and  $F_r^l$  covers a relatively large region since the output stride is set to 32 in our feature encoder. Thus, we can form the correlation as object-level correspondence, which is closely related to object appearance. We generate the pseudo labels of global correlation distillation by computing the global correlation  $a_{i,j}^t$  for each query with teacher  $\phi_t$ . The global correlation distillation loss  $\mathcal{L}_{gc}$  is defined to minimize the mean squared error between  $a$  and  $a^t$ .

$$\mathcal{L}_{gc} = \|a - a^t\|_2^2, \quad (3)$$

### 3.2 Temporal Feature Learning

We then perform temporal feature learning right after spatial feature learning. Temporal feature learning aims to learn the fine-grained correspondence between video frames. Recently, a few studies [20][38] introduce a reconstruction-based correspondence learning scheme, where each query pixel in the target frame can be reconstructed by leveraging the information of adjacent reference frames with a limited range. More specifically, the target and reference frame  $I_t, I_r$  are projected

157 into a fine-grained pixel embedding space. We denoted these embedding as  $F_t, F_r \in \mathbb{R}^{hw \times d}$ . For  
 158 each query pixel  $i$  in  $I_t$ , we can calculate the local correlation  $c_{i,j}$  w.r.t the reference frame in a local  
 159 range ( see the upper right of Figure 2 ):

$$c_{i,j} = \frac{\exp(F_t(i) \cdot F_r(j)/\tau)}{\sum_n \exp(F_t(i) \cdot F_r(n)/\tau)}, i \in \{1, \dots, hw\}, j, n \in \mathcal{N}(i), \quad (4)$$

160 Where  $\mathcal{N}(i)$  is the index set with a limited range of  $r$  pixels for pixel  $i$ . Then each query pixel  $i$  in  
 161 target frame can be reconstructed by a weighted-sum of pixels in  $\mathcal{N}(i)$ , according the local correlation  
 162 map  $c \in \mathbb{R}^{hw \times (r)^2}$ :

$$\hat{I}_t(i) = \sum_{j \in \mathcal{N}(i)} c_{i,j} I_r(j), \quad (5)$$

163 We regard the above process as a transformation function for all query pixels and denotes it as:  
 164  $\hat{I}_t = \mathcal{T}(c, I_r)$ . Then the reconstruction loss  $\mathcal{L}_{\text{rec}}$  is defined as L1 distance between  $\hat{I}_t$  and  $I_t$ .

$$\mathcal{L}_{\text{rec}} = \|I_t - \hat{I}_t\|_1, \quad (6)$$

165 However, the Eq 5 should only be applied when the feature embedding has the same size as video  
 166 frame. Thus the stride of  $\phi$  must be set to 1, which introduces large memory and computation cost.  
 167 One possible solution is to apply down-sampling on the target and reference frame. MAST [20]  
 168 proposes an image feature alignment module that samples the pixel at the center of strided convolution  
 169 kernels. However, down-sampling with a large rate would cause severe information loss and result  
 170 in more pixel occlusions between video frames, which obviously degrades the representation of  
 171 temporal feature learning. To address the issue, we design a pyramid learning framework consisting  
 172 of pyramid frame reconstruction and local correlation distillation with entropy-based selection.

173 **Pyramid frame reconstruction.** As you can see in Figure 2, we obtain a pair of feature pyramids  
 174  $\{F_t^l\}_{l=1}^{N-1}, \{F_r^l\}_{l=1}^{N-1}$ . Then we get the pyramid local correlation map  $\{c^l\}_{l=1}^{N-1}$  at each pyramid level  
 175 by utilizing Eq 4 with different range  $r^l$ . As the same time, we adopt a same down-sampling method  
 176 as [20] to get a pair of frame pyramids  $\{I_t^l\}_{l=1}^{N-1}, \{I_r^l\}_{l=1}^{N-1}$ , which has same shape with the feature  
 177 pyramids at each pyramid level. Given the  $c^l, I_t^l$  and  $I_r^l$ , we apply the pyramid reconstruction loss:

$$\mathcal{L}_{\text{rec}}^p = \sum_l \|I_t^l - \mathcal{T}(c^l, I_r^l)\|_1, \quad (7)$$

178 By doing this, we are able to exploit more free temporal supervision and get better temporal represen-  
 179 tation at the intermediate pyramid level.

180 **Local correlation distillation.** The bottom level of the frame pyramid contains rich information  
 181 and suffer less occlusions for temporal feature learning due to relatively small down-sampling  
 182 rate, which may result in more accurate local correlation map. Inspired by it, we design a novel  
 183 local correlation distillation loss which explicitly make constraint on the final local correlation map  
 184  $c^{N-1} \in \mathbb{R}^{h^{N-1} w^{N-1} \times (r^{N-1})^2}$ . We first compute the local correlation map  $c^{N-2}$  at level  $N-2$  and  
 185 then apply correlation down-sampling [34] to get pseudo labels  $c^t$  with the same size as  $c^{N-1}$ . Then  
 186 the local correlation distillation loss  $\mathcal{L}_{\text{lc}}$  is adopt to minimize the mean squared error between  $c^{N-1}$   
 187 and  $c^t$ .  
 188

189 **Entropy-based selection.** The correlation of each query w.r.t reference frame indicates more  
 190 uncertainty when having smooth distribution, which should be paid more attention to when applying  
 191 distillation. Thus we calculate the entropy for each query  $i$ :

$$\mathcal{H}(i) = \sum_j -\log c_{i,j}^{N-1}, \quad (8)$$

192 Then we obtain a mask  $m \in \mathbb{R}^{h^{N-1} w^{N-1}}$  to filter out the region with lower entropy by setting a  
 193 threshold  $T$ . The local correlation distillation loss with entropy selection is defined as:

$$\mathcal{L}_{\text{lc}}^e = \sum_i m_i \|c_{i,:}^{N-1} - c_{i,:}^t\|_2^2, \quad (9)$$

194 Eventually, our training loss of temporal feature learning is defined as:  $\mathcal{L}_t = \mathcal{L}_{\text{rec}}^p + \alpha \mathcal{L}_{\text{lc}}^e$ . The final  
 195 loss of training on video data is a weighted sum of  $\mathcal{L}_t$  and a regularization term  $\mathcal{L}_{\text{gc}}$  introduced in  
 196 Section 3.1:

$$\mathcal{L} = \mathcal{L}_t + \beta \mathcal{L}_{\text{gc}}, \quad (10)$$

## 4 Experiments

We verify the merit of our method in a series of correspondence-related tasks, including semi-supervised video object segmentation, pose keypoints tracking, and human parts segmentation propagation. This section will first introduce our experiment settings, including implementation and evaluation details. Then detailed ablation studies are performed to explain how each component of our method works. Last but not least, we finally report the performance comparison with state-of-the-art methods to further verify the effectiveness of our method.

### 4.1 Implementation Details

**Architectures.** We exploit the encoder  $\phi$  with both ResNet-18 and ResNet-50 [12] for self-supervised training. Following prior works [15][20][47], we reduce the stride of convolutional layers in  $\phi$  to increase the spatial resolution of feature maps on layer  $res_4$  by a factor of 4 or 8 (*i.e.*, downsampling rate 8 or 4). Furthermore, we set the stride of  $res_5$  layer to 4 in order to increase the receptive field for spatial feature learning.

**Training.** We first train our model using contrastive loss for 200 epochs on ImageNet [6] following most hyper-parameters settings of [13]. Then we perform temporal feature learning on YouTube-VOS [48] training set which consists of 3.5k videos. In this stage, the video frame is resized into  $256 \times 256$ , and channel-wise dropout in Lab color space [19][20] is adopted as the information bottleneck. We train the encoder for 90k/45k iterations with a mini-batch of 128/64 for ResNet-18/ResNet-50, using Adam as our optimizer. The initial learning rate is set to  $1e-4$  with a cosine (half-period) learning rate schedule. The frame reconstruction is applied on both  $res_3$  and  $res_4$  layer while we realize global correlation distillation on  $res_5$  layer.

**Evaluation.** We directly utilize the unsupervised pre-trained model as the feature extractor without any fine-tuning. Given the input frame with spatial resolution of  $H \times W$ , the evaluation is realized on the  $res_4$  layer with a spatial resolution of  $\frac{H}{8} \times \frac{W}{8}$  or  $\frac{H}{4} \times \frac{W}{4}$ . To propagate the semantic labels from the initial ground-truth annotation, the recurrent inference strategy is applied following recent works [15][20][47]. More specifically, the semantical label of the first frame, as well as previous predictions, are propagated to the current frame with the help of affinity between video frames. We evaluate our method over three downstream tasks including semi-supervised video object segmentation in DAVIS-2017 [32], human part propagation in VIP [53], and human pose tracking in JHMDB [17].

### 4.2 Ablation Study

The ablation study is performed with semi-supervised video object segmentation [32] on DAVIS-2017 validation set. Following the official protocol [32], we use the mean of region similarity  $\mathcal{J}_m$ , mean of contour accuracy  $\mathcal{F}_m$  and their average  $\mathcal{J} \& \mathcal{F}_m$  as the evaluation metrics. We conduct a series of experiments to prove the effectiveness of each component. The stride of the encoder is all set to 8 for training and evaluation.

**Temporal feature learning.** We first examine how each design in temporal feature learning impacts the overall performance, which is shown in Table 5 (a) 1 ~ 4. To have a clear look, we train the model from scratch on YouTube-VOS [48] when examining the efficacy of our components for temporal feature learning. The baseline is to apply frame reconstruction  $\mathcal{L}_{rec}$ . The  $p$ ,  $\mathcal{L}_{lc}$  and  $e$  represents pyramid frame reconstruction, local correlation distillation without and with entropy-based selection. From the table, we can see leveraging more supervision of frame reconstruction at each pyramid level leads to an improvement in the range of 0.8%. With the guidance of a more fine-grained local correlation map,  $\mathcal{L}_{lc}$  boosts up the accuracy from 65.4% to 68.1%. Moreover, enforcing the local correlation distillation to focus on the region with higher entropy leads to a performance gain in the range of 0.9%. By fusing the above components, the performance finally reaches 69.0%.

**Spatial feature learning.** We investigate the effect of training with each component in spatial feature learning. The results are shown in Table 3 (a) 5 ~ 6. With the help of the pre-training on ImageNet using contrastive loss, the performance of our method reaches 69.3%. Moreover, the global correlation distillation loss  $\mathcal{L}_{gc}$  boosts up the performance from 69.3% to 70.5% by keeping the ability of the model to capture object-level correspondence, which is closely related to object appearance modeling.

#	$\mathcal{L}_{nce}$	$\mathcal{L}_{gc}$	$\mathcal{L}_{rec}$	$p$	$\mathcal{L}_{lc}$	$e$	Dataset	Arch	$\mathcal{J} \& \mathcal{F}_m \uparrow$
1			✓				YTV	Res18	64.6
2			✓	✓			YTV	Res18	65.4
3			✓	✓	✓		YTV	Res18	68.1
4			✓	✓	✓	✓	YTV	Res18	69.0
5	✓		✓	✓	✓	✓	I + YTV	Res18	69.3
6	✓	✓	✓	✓	✓	✓	I + YTV	Res18	<b>70.5</b>

(a) Ablation study of each component.

Method	Dataset	Arch	$\mathcal{J} \& \mathcal{F}_m \uparrow$
$\mathcal{L}_{nce}$	I	Res50	66.5
w $\mathcal{L}_t$	I + YTV	Res50	69.6
w $\mathcal{L}_t$ + LwF [22]	I + YTV	Res50	69.9
w $\mathcal{L}_t$ + $\mathcal{L}_{gc}$	I + YTV	Res50	<b>71.3</b>

(b) Ablation study of  $\mathcal{L}_{gc}$ .

Table 5: **Ablation study for each component in our framework.** The "p" and "e" in (a) correspond to pyramid frame reconstruction and entropy-based selection. Models in (b) are all pre-trained on ImageNet with contrastive loss and models with "w" are subsequently trained on YouTube-VOS using different methods. I: ImageNet [6]. YTV: YouTube-VOS [48].



Figure 3: **Visualization of the ablation study.** Given a query point randomly sampled in the target frame, we visualize the result of computing the local correlation and global correlation map *w.r.t.* reference frame. The dashed line in red represents the range of computing correlation map *w.r.t.* query point. The reference frame is randomly sampled in the memory bank of inference strategy [15][20][47].

249 **Further exploitation of  $\mathcal{L}_{gc}$ .** Directly fine-tuning the model pre-trained with contrastive loss  $\mathcal{L}_{nce}$   
250 will lead to a well-known phenomenon of catastrophic forgetting [22], which is closely related to  
251 continual learning. To further verify the effectiveness of  $\mathcal{L}_{gc}$ , we exploit a general continual model  
252 LwF [22] based on knowledge distillation apart from directly fine-tuning on video dataset. We modify  
253 the framework of LwF to adapt to the paradigm of self-supervised learning and adopt [45] with  
254 ResNet-50 as our encoder, which has a stronger ability to capture object appearance. The results are  
255 shown on Table 5 (b). All methods achieve better results attributed to the proposed temporal feature  
256 learning, while our method using  $\mathcal{L}_{gc}$  gets the best performance. which indicates our method is able  
257 to build upon

258 **Further analysis.** We give a further analysis here based on the above experiments. On the one hand,  
259 temporal feature learning helps to learn the fine-grained correspondence related to motion estimation  
260 between frames, which is unable to accomplish by training an appearance model. As you can see in  
261 the first row of Figure 3, the appearance model trained with  $\mathcal{L}_{nce}$  is misled by two patches at different  
262 locations ( *i.e.* two feats of the tiger ) which has a similar appearance, while the model trained with  
263  $\mathcal{L}_t$  tends to learn a better temporal representation for fine-grained correspondence. However, in the  
264 second row of Figure 3, the model trained with  $\mathcal{L}_t$  fails to capture temporal correspondence with a  
265 local correlation when facing severe temporal discontinuity while the model trained with  $\mathcal{L}_{nce}$  is able  
266 to correct the mistakes by tracking the points based on the object appearance ( see with  $\mathcal{L}_{nce}$  and with  
267 all ).

### 268 4.3 Comparison with State-of-the-art

269 **Results for video object segmentation.** We compare our method against previous self-supervised  
270 methods in Table 3. For a fair comparison, we report both results by setting the stride of the encoder  
271 to 4 and 8. The results are all reported with layer  $res_4$  across all methods. Our method achieves  
272 state-of-the-art performance using both ResNet-18 and ResNet-50. For ResNet-18, our method with a  
273 stride of 8 achieves 70.5%, making an absolute performance improvement by 1.2% over all baselines  
274 using the same architecture. Benefiting from less information loss for temporal feature learning  
275 by setting the stride of the encoder to 4, the performance of our method reaches 73.1%, leading to  
276 a performance gain of 3.4% over MAMP [29], which consistently verify the idea of our methods.



Method	Sup.	Arch	Stride	Dataset		$\mathcal{J} \& \mathcal{F}_m \uparrow$	$\mathcal{J}_m \uparrow$	$\mathcal{F}_m \uparrow$
				Image	Video			
Supervised [12]	✓	ResNet-18	8	ImageNet	-	62.9	60.6	65.2
MoCo [13]		ResNet-18	8	ImageNet	-	60.8	58.6	63.1
SimSiam [5]		ResNet-18	8	ImageNet	-	62.0	60.0	64.0
Colorization [38]		ResNet-18	8	-	Kinetics	34.0	34.6	32.7
CorrFlow [19]		ResNet-18	8	-	OxUvA	50.3	48.4	52.2
MuG [26]		ResNet-18	8	-	OxUvA	54.3	52.6	56.1
UVC [21]		ResNet-18	8	COCO	Kinetics	59.5	57.7	61.3
ContrastCorr [39]		ResNet-18	8	COCO	TrackingNet	63.0	60.5	65.5
VFS [47]		ResNet-18	8	-	Kinetics	66.7	64.0	69.4
CRW [15]		ResNet-18	8	-	Kinetics	67.6	64.8	70.2
JSTG [52]		ResNet-18	8	-	Kinetics	68.7	65.8	71.6
DUL [1]		ResNet-18	8	-	YTV	69.3	67.1	71.6
MAST [20]		ResNet-18	4	-	YTV	65.5	63.3	67.6
MAMP [29]		ResNet-18	4	-	YTV	69.7	68.3	71.2
<b>Ours</b>		ResNet-18	8	-	YTV	69.0	66.4	71.7
<b>Ours</b>		ResNet-18	8	ImageNet	YTV	70.5	67.8	73.2
<b>Ours</b>		ResNet-18	4	-	YTV	71.2	68.9	73.8
<b>Ours</b>		ResNet-18	4	ImageNet	YTV	<b>73.1</b>	<b>70.4</b>	<b>75.9</b>
<hr/>								
Supervised [12]	✓	ResNet-50	8	ImageNet	-	66.0	63.7	68.4
MoCo [13]		ResNet-50	8	ImageNet	-	65.4	63.2	67.6
SimSiam [5]		ResNet-50	8	ImageNet	-	66.3	64.5	68.2
TimeCycle [41]		ResNet-50	8	-	VLOG	48.7	46.4	50.0
UVC [21]		ResNet-50	8	COCO	Kinetics	56.3	54.5	58.1
SeCo [51]		ResNet-50	8	-	Kinetics	60.6	60.4	62.8
VINCE [10]		ResNet-50	8	-	Kinetics	65.6	63.4	67.8
VFS [47]		ResNet-50	8	-	Kinetics	68.9	66.5	71.3
<b>Ours</b>		ResNet-50	8	ImageNet	YTV	<b>71.3</b>	<b>68.5</b>	<b>74.0</b>
<hr/>								
SiamMask [40]	✓	ResNet-50	-	I + C	YTV	56.4	54.3	58.5
OnAVOS [37]	✓	ResNet-38	-	I + C + P	D	65.4	61.6	69.1
OSVOS-S [27]	✓	VGG-16	-	I + P	D	68.0	64.7	71.3

Table 3: **Quantitative results for video object segmentation on validation set of DAVIS-2017 [32].** We show results of state-of-the-art self-supervised methods and some supervised methods for comparison. "Dataset" represents the dataset(s) for pre-training, including: I:ImageNet [6] (1.28m). C:COCO [23] (30k). O:OxUvA [35] (14h). T:TrackingNet [30] (300h). K:Kinetics [4] (800h). V:VLOG [9] (344h). YTV:YouTube-VOS [48] (5h). D:DAVIS-2017 [32] (-). P:PASCAL-VOC [8] (-). We report the data size for self-supervised methods ( total number/duration of image/video dataset ).

Besides, we found our method trained with only temporal feature learning reaches 69.0%/71.2% with a stride of 8/4, surpassing all methods pre-trained on Kinetics [4] or TrackingNet [30] which has a much bigger size than YouTube-VOS [48]. For ResNet-50, our method still outperforms VFS [47] by 2.4%. More remarkably, our method even outperforms some task-specific fully-supervised algorithms [40][37][27].

### Results for human part propagation.

Next, we evaluate our method for human part tracking. Experiments are conducted on the validation set of VIP [53], which consists of 50 videos with 19 human semantic part classes, requiring more precise matching than DAVIS-2017 [32]. Following [53], we adopt mean intersection-over-union (mIoU) as our evaluation metric and resize the video frames to  $560 \times 560$ . All models except TimeCycle [41] are set to ResNet-18 with a stride of 8 for a fair comparison. The results are shown in Table 2. Our method achieves state-of-the-art performance, surpassing all previous state-of-the-art by 0.8%. Notably, our model outperforms ATEN [53] which is specifically designed for the task using human annotations. Figure 4 (b) depicts some visualization results on several representative videos.

Methods	Sup.	VIP		JHMDB	
		mIoU $\uparrow$	PCK@0.1 $\uparrow$	PCK@0.2 $\uparrow$	
ResNet-18 [12]	✓	31.9	53.8	74.6	
TimeCycle [41]		28.9	57.3	78.1	
UVC [21]		34.1	58.6	79.6	
CRW [15]		38.6	59.3	80.3	
ContrastCorr [39]		37.4	61.1	80.8	
VFS [47]		39.9	60.5	79.5	
CLTC [16]		37.8	60.5	82.3	
JSTG [52]		40.2	61.4	<b>85.3</b>	
<b>Ours</b>		<b>41.0</b>	<b>63.1</b>	82.9	
<hr/>					
ATEN [53]	✓	37.9	-	-	
Thin-Slicing Net [33]	✓	-	68.7	92.1	

Table 2: **Quantitative results for human part propagation and human pose tracking.** We show results of state-of-the-art self-supervised methods and some supervised methods for comparison.



(a) Video Object Segmentation (1-4 objects)



(b) Human Part Propagation (20 parts)



(c) Pose Keypoint Tracking (15 key points)



Figure 4: Qualitative results for label propagation. Given the first frame with different annotations highlighted with a blue outline, we propagate it to the current frame without fine-tuning. (a) Video object segmentation on DAVIS-2017 [32]. (b) Human part propagation on VIP [53]. (c) Pose keypoint tracking on JHMDB [17].

**Results for human pose tracking.** We then make a performance comparison on the downstream task of human pose tracking. We conduct the experiments on the validation of JHMDB [17] which has 268 videos. The annotations consist of 15 body joints for each person. The probability of correct keypoint [50] is utilized here to examine the accuracy between result and ground truth with different thresholds. Follow the evaluation protocol of [15][21], we resize the video frames to  $320 \times 320$ . The results in Table 2 show a consistent performance gain over previous methods, which successfully demonstrates the transferability of our method to different downstream tasks. The visualization results in Figure 4 (c) show the robustness of our approach to various challenges.

## 5 Conclusions

In this work, we look into the self-supervised video correspondence learning from two perspectives: (1) Learning an appearance model invariant for appearance changes. (2) Learning a better temporal representation to capture fine-grained correspondence between video frames. To materialize our idea, we design a novel framework that learns the spatial and temporal feature sequentially. More specifically, we first train a model using contrastive loss on ImageNet. Then temporal feature learning is performed with the objective of frame reconstruction. To achieve the goal of realizing fine-grained matching and maintaining spatial representation at the same time, we devise a pyramid learning framework consisting of local and global correlation distillation. The distillation of local correlation is achieved between the different pyramid levels since the bottom level always contains richer information for temporal feature learning, while the global correlation distillation is conducted at the coarse pyramid level, which is closely related to finding the correspondence at the object-level. Furthermore, the entropy-based selection is proposed to pay more attention to the region with high uncertainty when applying the local correlation distillation. Extensive experiments on a variety of downstream tasks validate our method. More remarkably, self-supervised training shows superior performance to fully-supervised ImageNet pre-training and several dedicated methods with task-specific human annotations.

## References

- [1] N. Araslanov, S. Schaub-Meyer, and S. Roth. Dense unsupervised learning for video segmentation. In *NeurIPS*, 2021.
- [2] S. Caelles, K.-K. Maninis, J. Pont-Tuset, L. Leal-Taixé, D. Cremers, and L. Van Gool. One-shot video object segmentation. In *CVPR*, 2017.
- [3] M. Caron, I. Misra, J. Mairal, P. Goyal, P. Bojanowski, and A. Joulin. Unsupervised learning of visual features by contrasting cluster assignments. In *NeurIPS*, 2020.
- [4] J. Carreira and A. Zisserman. Quo vadis, action recognition? a new model and the kinetics dataset. In *CVPR*, 2017.
- [5] X. Chen and K. He. Exploring simple siamese representation learning. In *CVPR*, 2021.
- [6] J. Deng. A large-scale hierarchical image database. In *CVPR*, 2009.
- [7] A. Dosovitskiy, P. Fischer, E. Ilg, P. Hausser, C. Hazirbas, V. Golkov, P. Van Der Smagt, D. Cremers, and T. Brox. FlowNet: Learning optical flow with convolutional networks. In *ICCV*, 2015.
- [8] M. Everingham, S. Eslami, L. Van Gool, C. K. Williams, J. Winn, and A. Zisserman. The pascal visual object classes challenge: A retrospective. *International journal of computer vision*, 2015.
- [9] D. F. Fouhey, W.-c. Kuo, A. A. Efros, and J. Malik. From lifestyle vlogs to everyday interactions. In *CVPR*, 2018.
- [10] D. Gordon, K. Ehsani, D. Fox, and A. Farhadi. Watching the world go by: Representation learning from unlabeled videos. *arXiv preprint arXiv:2003.07990*, 2020.
- [11] J.-B. Grill, F. Strub, F. Altché, C. Tallec, P. Richemond, E. Buchatskaya, C. Doersch, B. Avila Pires, Z. Guo, M. Gheshlaghi Azar, et al. Bootstrap your own latent-a new approach to self-supervised learning. In *NeurIPS*, 2020.
- [12] K. He, X. Zhang, S. Ren, and J. Sun. Deep residual learning for image recognition. In *CVPR*, 2016.
- [13] K. He, H. Fan, Y. Wu, S. Xie, and R. Girshick. Momentum contrast for unsupervised visual representation learning. In *CVPR*, 2020.
- [14] B. K. Horn and B. G. Schunck. Determining optical flow. *Artificial intelligence*, 1981.
- [15] A. Jabri, A. Owens, and A. Efros. Space-time correspondence as a contrastive random walk. In *NeurIPS*, 2020.
- [16] S. Jeon, D. Min, S. Kim, and K. Sohn. Mining better samples for contrastive learning of temporal correspondence. In *CVPR*, 2021.
- [17] H. Jhuang, J. Gall, S. Zuffi, C. Schmid, and M. J. Black. Towards understanding action recognition. In *ICCV*, 2013.
- [18] R. Jonschkowski, A. Stone, J. T. Barron, A. Gordon, K. Konolige, and A. Angelova. What matters in unsupervised optical flow. In *ECCV*, 2020.
- [19] Z. Lai and W. Xie. Self-supervised learning for video correspondence flow. In *BMVC*, 2019.
- [20] Z. Lai, E. Lu, and W. Xie. Mast: A memory-augmented self-supervised tracker. In *CVPR*, 2020.
- [21] X. Li, S. Liu, S. De Mello, X. Wang, J. Kautz, and M.-H. Yang. Joint-task self-supervised learning for temporal correspondence. In *NeurIPS*, 2019.
- [22] Z. Li and D. Hoiem. Learning without forgetting. *IEEE transactions on PAMI*, 2017.
- [23] T.-Y. Lin, M. Maire, S. Belongie, J. Hays, P. Perona, D. Ramanan, P. Dollár, and C. L. Zitnick. Microsoft coco: Common objects in context. In *ECCV*, 2014.
- [24] L. Liu, J. Zhang, R. He, Y. Liu, Y. Wang, Y. Tai, D. Luo, C. Wang, J. Li, and F. Huang. Learning by analogy: Reliable supervision from transformations for unsupervised optical flow estimation. In *CVPR*, 2020.
- [25] P. Liu, I. King, M. R. Lyu, and J. Xu. Ddflow: Learning optical flow with unlabeled data distillation. In *AAAI*, 2019.

[26] X. Lu, W. Wang, J. Shen, Y.-W. Tai, D. J. Crandall, and S. C. Hoi. Learning video object segmentation from unlabeled videos. In *CVPR*, 2020.

[27] K.-K. Maninis, S. Caelles, Y. Chen, J. Pont-Tuset, L. Leal-Taixé, D. Cremers, and L. Van Gool. Video object segmentation without temporal information. *IEEE transactions on PAMI*, 2018.

[28] S. Meister, J. Hur, and S. Roth. Unflow: Unsupervised learning of optical flow with a bidirectional census loss. In *AAAI*, 2018.

[29] B. Miao, M. Bennamoun, Y. Gao, and A. Mian. Self-supervised video object segmentation by motion-aware mask propagation. *arXiv preprint arXiv:2107.12569*, 2021.

[30] M. Muller, A. Bibi, S. Giancola, S. Alsubaihi, and B. Ghanem. Trackingnet: A large-scale dataset and benchmark for object tracking in the wild. In *ECCV*, 2018.

[31] S. W. Oh, J.-Y. Lee, N. Xu, and S. J. Kim. Video object segmentation using space-time memory networks. In *ICCV*, 2019.

[32] J. Pont-Tuset, F. Perazzi, S. Caelles, P. Arbeláez, A. Sorkine-Hornung, and L. Van Gool. The 2017 davis challenge on video object segmentation. *arXiv preprint arXiv:1704.00675*, 2017.

[33] J. Song, L. Wang, L. Van Gool, and O. Hilliges. Thin-slicing network: A deep structured model for pose estimation in videos. In *CVPR*, 2017.

[34] Z. Teed and J. Deng. Raft: Recurrent all-pairs field transforms for optical flow. In *ECCV*, 2020.

[35] J. Valmadre, L. Bertinetto, J. F. Henriques, R. Tao, A. Vedaldi, A. W. Smeulders, P. H. Torr, and E. Gavves. Long-term tracking in the wild: A benchmark. In *ECCV*, 2018.

[36] A. Van den Oord, Y. Li, and O. Vinyals. Representation learning with contrastive predictive coding. *arXiv e-prints*, pages arXiv–1807, 2018.

[37] P. Voigtlaender and B. Leibe. Online adaptation of convolutional neural networks for video object segmentation. *arXiv preprint arXiv:1706.09364*, 2017.

[38] C. Vondrick, A. Shrivastava, A. Fathi, S. Guadarrama, and K. Murphy. Tracking emerges by colorizing videos. In *ECCV*, 2018.

[39] N. Wang, W. Zhou, and H. Li. Contrastive transformation for self-supervised correspondence learning. In *AAAI*, 2020.

[40] Q. Wang, L. Zhang, L. Bertinetto, W. Hu, and P. H. Torr. Fast online object tracking and segmentation: A unifying approach. In *CVPR*, 2019.

[41] X. Wang, A. Jabri, and A. A. Efros. Learning correspondence from the cycle-consistency of time. In *CVPR*, 2019.

[42] X. Wang, R. Zhang, C. Shen, T. Kong, and L. Li. Dense contrastive learning for self-supervised visual pre-training. In *CVPR*, 2021.

[43] Z. Wang, H. Zhao, Y.-L. Li, S. Wang, P. Torr, and L. Bertinetto. Do different tracking tasks require different appearance models? In *NeurIPS*, 2021.

[44] Z. Wu, Y. Xiong, S. X. Yu, and D. Lin. Unsupervised feature learning via non-parametric instance discrimination. In *CVPR*, 2018.

[45] E. Xie, J. Ding, W. Wang, X. Zhan, H. Xu, P. Sun, Z. Li, and P. Luo. Detco: Unsupervised contrastive learning for object detection. In *ICCV*, 2021.

[46] Y. Xiu, J. Li, H. Wang, Y. Fang, and C. Lu. Pose flow: Efficient online pose tracking. In *BMVC*, 2018.

[47] J. Xu and X. Wang. Rethinking self-supervised correspondence learning: A video frame-level similarity perspective. In *ICCV*, 2021.

[48] N. Xu, L. Yang, Y. Fan, D. Yue, Y. Liang, J. Yang, and T. Huang. Youtube-vos: A large-scale video object segmentation benchmark. *arXiv preprint arXiv:1809.03327*, 2018.

[49] C. Yang, Z. Wu, B. Zhou, and S. Lin. Instance localization for self-supervised detection pretraining. In *CVPR*, 2021.

- 417 [50] Y. Yang and D. Ramanan. Articulated human detection with flexible mixtures of parts. *IEEE transactions*  
418 *on PAMI*, 2012.
- 419 [51] T. Yao, Y. Zhang, Z. Qiu, Y. Pan, and T. Mei. Seco: Exploring sequence supervision for unsupervised  
420 representation learning. In *AAAI*, 2021.
- 421 [52] Z. Zhao, Y. Jin, and P.-A. Heng. Modelling neighbor relation in joint space-time graph for video correspon-  
422 dence learning. In *ICCV*, 2021.
- 423 [53] Q. Zhou, X. Liang, K. Gong, and L. Lin. Adaptive temporal encoding network for video instance-level  
424 human parsing. In *ACM MM*, 2018.

## 425 Checklist

426 The checklist follows the references. Please read the checklist guidelines carefully for information on  
427 how to answer these questions. For each question, change the default **[TODO]** to **[Yes]** , **[No]** , or  
428 **[N/A]** . You are strongly encouraged to include a **justification to your answer**, either by referencing  
429 the appropriate section of your paper or providing a brief inline description. For example:

- 430 • Did you include the license to the code and datasets? **[Yes]**
- 431 • Did you include the license to the code and datasets? **[No]** The code and the data are  
432 proprietary.
- 433 • Did you include the license to the code and datasets? **[N/A]**

434 Please do not modify the questions and only use the provided macros for your answers. Note that the  
435 Checklist section does not count towards the page limit. In your paper, please delete this instructions  
436 block and only keep the Checklist section heading above along with the questions/answers below.

- 437 1. For all authors...
- 438 (a) Do the main claims made in the abstract and introduction accurately reflect the paper’s  
439 contributions and scope? **[TODO]**
- 440 (b) Did you describe the limitations of your work? **[TODO]**
- 441 (c) Did you discuss any potential negative societal impacts of your work? **[TODO]**
- 442 (d) Have you read the ethics review guidelines and ensured that your paper conforms to  
443 them? **[TODO]**
- 444 2. If you are including theoretical results...
- 445 (a) Did you state the full set of assumptions of all theoretical results? **[TODO]**
- 446 (b) Did you include complete proofs of all theoretical results? **[TODO]**
- 447 3. If you ran experiments...
- 448 (a) Did you include the code, data, and instructions needed to reproduce the main experi-  
449 mental results (either in the supplemental material or as a URL)? **[TODO]**
- 450 (b) Did you specify all the training details (e.g., data splits, hyperparameters, how they  
451 were chosen)? **[TODO]**
- 452 (c) Did you report error bars (e.g., with respect to the random seed after running experi-  
453 ments multiple times)? **[TODO]**
- 454 (d) Did you include the total amount of compute and the type of resources used (e.g., type  
455 of GPUs, internal cluster, or cloud provider)? **[TODO]**
- 456 4. If you are using existing assets (e.g., code, data, models) or curating/releasing new assets...
- 457 (a) If your work uses existing assets, did you cite the creators? **[TODO]**
- 458 (b) Did you mention the license of the assets? **[TODO]**
- 459 (c) Did you include any new assets either in the supplemental material or as a URL?  
460 **[TODO]**
- 461 (d) Did you discuss whether and how consent was obtained from people whose data you’re  
462 using/curating? **[TODO]**

- 463 (e) Did you discuss whether the data you are using/curating contains personally identifiable  
464 information or offensive content? **[TODO]**
- 465 5. If you used crowdsourcing or conducted research with human subjects...
- 466 (a) Did you include the full text of instructions given to participants and screenshots, if  
467 applicable? **[TODO]**
- 468 (b) Did you describe any potential participant risks, with links to Institutional Review  
469 Board (IRB) approvals, if applicable? **[TODO]**
- 470 (c) Did you include the estimated hourly wage paid to participants and the total amount  
471 spent on participant compensation? **[TODO]**